ISSN: 2277-3754
ISO 9001:2008 Certified
International Journal of Engineering and Innovative Technology (IJEIT)
Volume 3, Issue 3, September 2013

Practical Realization of Complex Wavelet Transform Based Filter for Image Fusion and De-noising

Rudra Pratap Singh Chauhan, Dr. Rajiva Dwivedi

Abstract*—Image fusion is the process of extracting meaningful visual information from two or more images and combining them to form one fused image. In many real life applications such as remote sensing and medical image diagnosis image fusion plays imperative role and it is more popular for image processing applications. Previously, real valued wavelet transforms have been used for image fusion. But the Discrete wavelet transform (DWT) suffers from the shift variance and lack of directionality associated with its wavelet bases. These problems have been overcome by the use of a reversible and discrete complex wavelet transform (the Dual Tree Complex Wavelet Transform DT-CWT). However, the existing structure of this complex wavelet decomposition enforces a very strict choice of filters in order to achieve a necessary quarter shift in coefficient output. This paper therefore introduces an alternative structure to the DTCWT that is more flexible in its potential choice of filters and can be implemented by the combination of four normally structured wavelet transforms. The use of these more common wavelet transforms enables this method to make use of existing optimized wavelet decomposition and recomposition methods, code and filter choice.

***Index Terms*—Complex Wavelet Transform, Discrete Wavelet Transform, Image Fusion, Wavelet.**

I. INTRODUCTION

Image fusion means in general an significant approach to extraction of information acquired in several domains. The goal of image fusion (IF) is to integrate complementary multi-sensor, multi-temporal and/or multi-view information into one new image containing information the quality of which cannot be achieved otherwise. The term quality, its meaning and measurement depend on the particular application. Image fusion has been used in many application areas. In remote sensing and in astronomy, multisensory fusion is used to achieve high spatial and spectral resolutions by combining images from two sensors, one of which has high spatial resolution and the other one high spectral resolution. Numerous fusion applications have appeared in medical imaging like simultaneous evaluation of CT, MRI, and/or PET images. Plenty of applications which use multi-sensor fusion of visible and infrared images have appeared in military, security, and surveillance areas. In the case of multi-view fusion, a set of images of the same scene taken by the same sensor but from different viewpoints is fused to obtain an image with higher resolution than the sensor normally provides or to recover the 3D representation of the scene. The multi-temporal approach recognizes two different aims. Images of the same scene are acquired at different times either to find and evaluate changes in the scene or to obtain a less degraded image of the scene. The former aim is common in medical imaging, especially in change detection of organs and tumors, and in remote sensing for monitoring land or forest exploitation. The acquisition period is usually months or years. The latter aim requires the different measurements to be much closer to each other, typically in the scale of seconds, and possibly under different conditions. The list of applications mentioned above illustrates the diversity of problems we face when fusing images. It is impossible to design a universal method applicable to all image fusion tasks. Every method should take into account not only the fusion purpose and the characteristics of individual sensors, but also particular imaging conditions, imaging geometry, noise corruption, required accuracy and application-dependent data properties.

II. WAVELET TRANSFORM

The wavelet transform, originally developed in the mid 80’s, is a signal analysis tool that provides a multi-resolution decomposition of an image in a bi-orthogonal basis and results in a non-redundant image representation. This basis are called wavelets, and they are functions generated from one single function, called mother wavelet, by dilations and translations. Although this is not a new idea, what makes this transformation more suitable than other transformations such as the Fourier Transform or the Discrete Cosine Transform, is the ability of representing signal features in both time and frequency domain. Figure 2-5 shows an implementation of the discrete wavelet transform. In this filter bank, the input signal goes through two one-dimensional digital filters. One of them, *H0*, performs a high pass filtering operation and the other *H1* a low pass one.

Each filtering operation is followed by sub-sampling by a factor of 2. Then, the signal is reconstructed by first up-sampling, then filtering and summing the sub-bands. The synthesis filters *F0* and *F1* must be specially adapted to the analysis filters *H0* and *H1* to achieve perfect reconstruction [1]. By considering the z-transfer function of the 2-chanel filter bank shown in Figure 2-5 it is easy to obtain the relationship that those filters need to satisfy. After analysis, the two sub bands are:

ISSN: 2277-3754
ISO 9001:2008 Certified
International Journal of Engineering and Innovative Technology (IJEIT)
Volume 3, Issue 3, September 2013

$$\frac{1}{2}\left[H_0\left(z^{1/2}\right)X\left(z^{1/2}\right)+H_0\left(-z^{1/2}\right)X\left(-z^{1/2}\right)\right] \quad (1)$$

$$\frac{1}{2}\left[H_1\left(z^{1/2}\right)X\left(z^{1/2}\right)+H_1\left(-z^{1/2}\right)X\left(-z^{1/2}\right)\right] \quad (2)$$

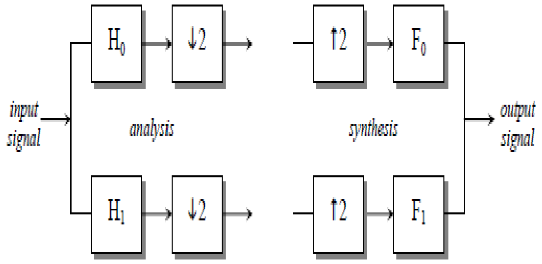

Fig 1: Two Channel Filter Bank Structure

Then, the filter bank combines the channels to get $x\hat{}(n)$. In the z-domain this is $X\hat{}(z)$. Half of the terms involve $X(z)$ and half involve $X(-z)$.

$$\hat{X}(z)=\frac{1}{2}\left[F_0(z)H_0(z)+F_1(z)H_1(z)\right]X(z)+ \\ +\frac{1}{2}\left[F_0(z)H_0(-z)+F_1(z)H_1(-z)\right]X(-z) \quad (3)$$

There are two factors to eliminate: aliasing and distortion. For alias cancellation choose:

$$F_0(z)=H_1(-z) \quad (4)$$

$$F_1(z)=-H_0(-z) \quad (5)$$

The distortion must be reduced to a delay term, to achieve this Smith and Barnwell suggested [3]:

$$H_1(z)=-z^{-N}H_0(-z^{-1}) \quad (6)$$

With these restrictions the final filtering equation is:

$$\hat{X}(z)=\frac{1}{2}z^{-N}\left[H_0(z)H_0(z^{-1})+H_0(-z^{-1})H_0(z)\right]X(z) \quad (7)$$

Figure 2 represents one step in a multiscale pyramid decomposition of an image [2]. The algorithm applies a one-dimensional high and low pass filtering step to the rows and columns separately in the input image. The inverse transform filter bank structure is represented in Figure 3.

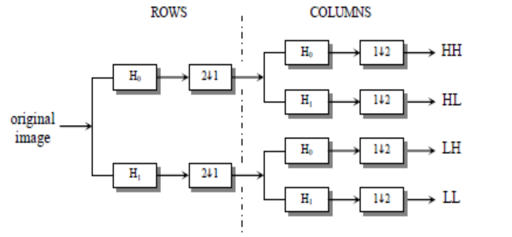

Fig 2: Filter bank structure of DWT analysis

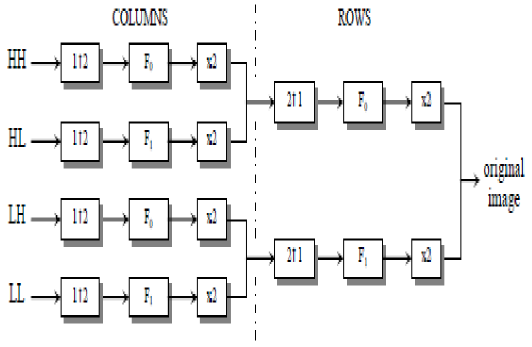

Fig 3: Filter bank structure of the inverse DWT synthesis

Successive application of this decomposition to the LL sub-band gives rise to pyramid decomposition where the sub-images correspond to different resolution levels and orientations as exemplified in Figure 4. Some images decomposed with the wavelet transform are shown in Figure5.

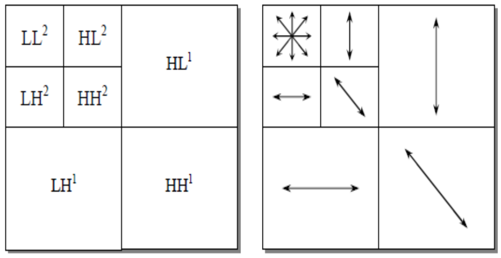

Fig 4: Image decomposition. Each sub-band has a natural orientation

Image (a)

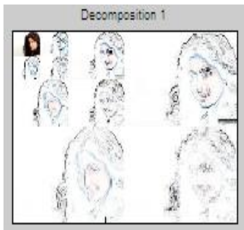

Image (b)

Image (c)

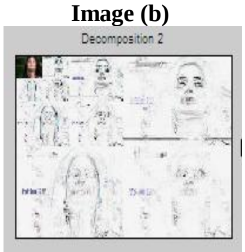

Image (d)

Fig 5: Images (a) and (c) shows original images and (b) and (d) their wavelet decomposition.

ISSN: 2277-3754
ISO 9001:2008 Certified
International Journal of Engineering and Innovative Technology (IJEIT)
Volume 3, Issue 3, September 2013

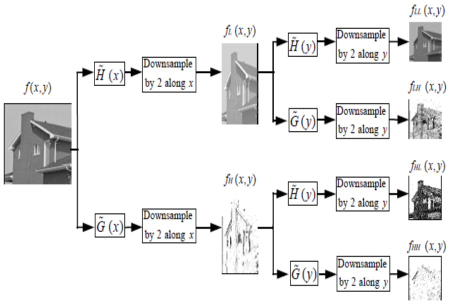

Fig 6: Forward Wavelet Transform (Analysis Filter)

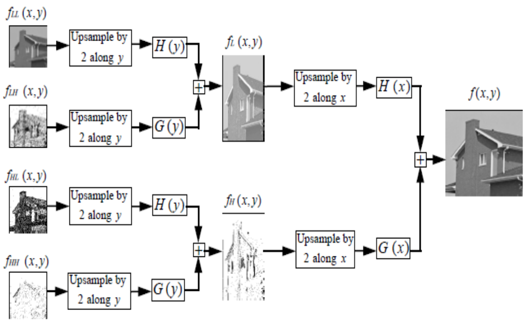

Fig 7: Inverse Wavelet Transform (Synthesis Filter)

III. COMPLEX WAVELET TRANSFORM

The wavelet transform has established an impressive reputation as a tool for this, especially for images and motion video. Many researchers have also tried to use wavelets for signal analysis and reconstruction but the results have tended to be disappointing. Here we consider possible reasons for this and propose the dual-tree *complex* wavelet transform as a useful tool for overcoming some of these problems. The Discrete Wavelet Transform (DWT) is most commonly used in its maximally decimated form (Mallat's dyadic filter tree [4]). This works well for compression but its use for other signal analysis and reconstruction tasks has been hampered by two main disadvantages:

- Lack of *shift invariance*, which means that small shifts in the input signal can cause major variations in the distribution of energy between DWT coefficients at different scales.
- Poor *directional selectivity* for diagonal features, because the wavelet filters are separable and real.

Here, we introduced a more computationally efficient approach to shift invariance, the Dual-Tree Complex Wavelet Transform (DT CWT)[5,6]. Furthermore the DT CWT also gives much better directional selectivity when filtering multidimensional signals. In summary, it has the following properties:

- Approximate shift invariance;
- Good directional selectivity in 2-dimensions (2-D) with Gabor-like filters (also true for higher dimensionality, *m*-D);
- Perfect reconstruction (PR) using short linear-phase filters;
- Limited redundancy, independent of the number of scales, 2 : 1 for 1-D (2^m : 1 for *m*-D); Efficient order-*N* computation – only twice the simple DWT for 1-D (2*m* times for *m*-D). In [7] we proposed a way of analyzing the shift invariant properties of the DT CWT and here we expand on these basic ideas and develop them somewhat further. Another approach both to shift invariance and to directional selectivity was pioneered by Simoncelli et al. [4], and was based on Laplacian pyramids and steerable filters, designed in the frequency domain. The complex wavelet methods, presented here, are believed to offer some useful alternative properties to these – principally perfect reconstruction and greater directional selectivity.

IV. THE DUAL TREE COMPLEX WAVELET TRANSFORM

The use of complex wavelets [5, 8] for motion estimation and showed that complex wavelets could provide approximate shift invariance. Unfortunately we were unable to obtain PR and good frequency characteristics using short support complex FIR filters in a single tree (eg. fig. 8 Tree *a*). However we observed that we can also achieve approximate shift invariance with a *real* DWT, by doubling the sampling rate at each level of the tree. For this to work, the samples must be evenly spaced. One way to double all the sampling rates in a conventional wavelet tree, such as Tree *a* of fig. 8, is to eliminate the down-sampling by 2 after the level 1 filters, H_{0a} and H_{1a}. This is equivalent to having two parallel fully-decimated trees, *a* and *b* in fig. 8, provided that the delays of filters H_{0b} and H_{1b} are one sample offset from the delays of H_{0a} and H_{1a}, which ensures that the level 1 down samplers in tree *b* pick the opposite samples to those in tree *a*. We then find that, to get uniform intervals between samples from the two trees *below* level 1, the filters in one tree must provide delays that are *half a sample* different (at each filter's input rate) from those in the opposite tree.

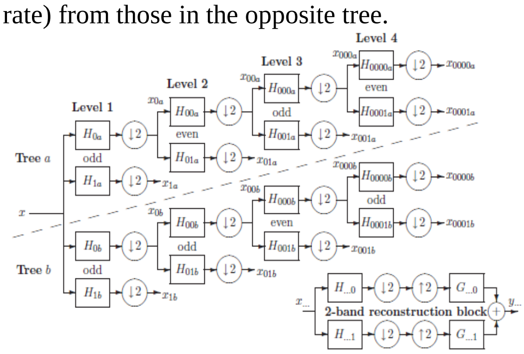

Fig 8: The Dual-Tree Complex Wavelet Transform (DT CWT), comprising two trees of real filters, *a* and *b*, which produce the real and imaginary parts of the complex coefficients. Odd and even length biorthogonal linear-phase filters are placed as shown to achieve the correct relative signal delays.

For linear phase filters, this requires *odd-length* filters in one tree and *even-length* filters in the other. Greater symmetry between the two trees occurs if each tree uses odd and even filters alternately from level to level, but this is not essential. In fig. 2a we show the positions of the wavelet basis functions

ISSN: 2277-3754
ISO 9001:2008 Certified
International Journal of Engineering and Innovative Technology (IJEIT)
Volume 3, Issue 3, September 2013

when the filters are arranged to be odd and even as in fig. 8. Note the vertical alignment of these bases at each scale, such that the tree *b* scaling functions interpolate midway between those of tree *a*, while the tree *b* wavelets are aligned with those of tree *a* but with a quadrature phase shift in the underlying oscillation. To invert the DT CWT, each tree in fig. 8 is inverted separately using biorthogonal filters *G:::*, designed for perfect reconstruction with the corresponding analysis filters *H:::* in the 2-band reconstruction block, shown lower right. Finally the two tree outputs are averaged in order to obtain an approximately shift invariant system. This system is a wavelet *frame* [2] with redundancy two; and if the filters are designed such that the analysis and reconstruction filters have very similar frequency responses (i.e. are almost orthogonal, as is the case for the filters given later in Table 1), then it is an almost tight frame, which means that energy is approximately preserved when signals are transformed into the DT CWT domain. The basis functions in fig. 2a were obtained by injecting unit pulses separately into the inverse DT CWT at each scale in turn. The real and imaginary parts were obtained by injecting the unit pulses into trees *a* and *b* in turn.

V. ODD/EVEN FILTER DESIGN METHOD

We first suggest a way to design filters for the odd/even DT CWT which achieve good shift invariance. For the low pass filters, equation (2) implies that the tree *b* samples should interpolate midway between the tree *a* samples, effectively doubling the sampling rate, as shown in fig 2. This may be achieved by two identical odd-length low pass filters at level 1, offset by 1 sample delay, and then by pairs of odd and even length filters at further levels to achieve an extra delay difference of $M/4$ samples, so as to make the total delay difference $M/2$ samples at each level *m*, where $M = 2^m$. The responses of $A(z)$ and $B(z)$ also need to match, which can only be achieved approximately for odd/even filters beyond level 1. We do this by designing the even-length filter H_{00a} to give minimum mean squared error in the approximation

$$z^{-2}\, H_{0a}(z)\, H_{00a}(z^2) \approx H_{0b}(z)\, H_{00b}(z^2)$$

(8)

Where H_{00b} is assumed to be the same odd-length design as the two level 1 filters, such that $H_{00b}(z) = H_{0b}(z) = z^{-1}H_{0a}(z)$. In this case solving for H_{00a} is just a matrix pseudo-inverse problem. Then the high pass filter H_{01a} can be designed to form a perfect reconstruction set with H_{00a} such that the reconstruction filters G_{00a} and G_{00b} also match each other closely. Finally the symmetry of the odd-length high pass filters and the anti-symmetry of the even-length high pass filters produce the required phase relationships between the positive and negative frequency pass bands, and equations (3) are approximately satisfied too. These odd and even length filters can then be used for all subsequent levels of the transform, in accordance with fig. 1. Good shift invariance (and wavelet smoothness) requires that frequency response side lobes of the cascaded multirate filters should be small. This is achieved if each low pass filter has a stop band covering $\frac{1}{3}$ to $\frac{2}{3}$ of its sample rate, so as to reject the image frequencies due to sub sampling in the next low pass stage. If the high pass filters then mirror this characteristic, the conditions for no overlap of the shifted band pass responses in equation (4) are automatically satisfied. To illustrate this process, we have designed two linear-phase PR biorthogonal filter sets which meet the above conditions quite well and are also nearly orthogonal. For the odd length set, we designed (13,19)-tap filters using the (1-D) transformation of variables method [8]. Then for the even-length set, we designed a (12,16)-tap even-length set to minimize the error in equation (6). The analysis filter coefficients are listed in Table 1 (the reconstruction filters are obtained by negating alternate coefficients and swapping bands). These filters may be implemented efficiently using ladder structures, the odd filter pair requiring 4 multiplies and 6 additions per input sample, and the even pair 7.5 multiplies and 7 additions. Fig. 6 shows the frequency responses of a 4-level reconstruction filter bank when the coefficients from the two trees are combined to form complex coefficients (the scaling function coefficients are also combined in this way). The analysis filters are very similar. Note the absence of gain at negative frequencies. We have implemented these filters and have found them to be good for many applications. However other options do exist, as any combination of odd length and even-length biorthogonal linear phase filters could in theory be used, although with varying levels of shift invariance and wavelet smoothness.

Table 1: Coefficients of the (13, 19)-tap and (12, 16)-tap odd/even filters

odd $H_{...0}$ 13-tap	odd $H_{...1}$ 19-tap	even $H_{...0}$ 12-tap	even $H_{...1}$ 16-tap
	-0.0000706		
	0		-0.0004645
-0.0017581	0.0013419		0.0013349
0	-0.0018834	-0.0058109	0.0022006
0.0222656	-0.0071568	0.0166977	-0.0130127
-0.0468750	0.0238560	-0.0000641	0.0015360
-0.0482422	0.0556431	-0.0834914	0.0869008
0.2968750	-0.0516881	0.0919537	0.0833552
0.5554688	-0.2997576	0.4807151	-0.4885957
0.2968750	0.5594308	0.4807151	0.4885957
-0.0482422	-0.2997576	0.0919537	-0.0833552
⋮	⋮	⋮	⋮

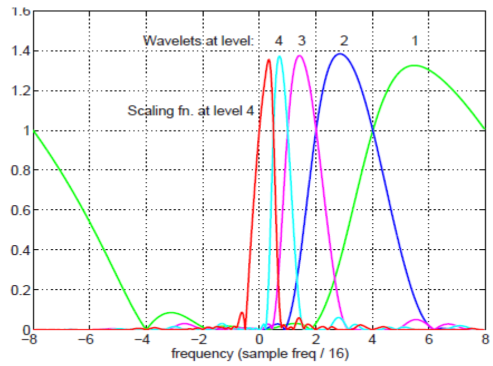

Fig 9: Frequency responses of complex wavelets at levels 1 to 4 and of the level 4 scaling function.

ISSN: 2277-3754
ISO 9001:2008 Certified
International Journal of Engineering and Innovative Technology (IJEIT)
Volume 3, Issue 3, September 2013

VI. EXTENSION TO M-DIMENSIONS

Extension of the DT CWT to two dimensions is achieved by separable filtering along columns and then rows. However, if column and row filters both suppress negative frequencies, then only the first quadrant of the 2-D signal spectrum is retained. It is well known from 2- D Fourier transform theory, that two adjacent quadrants of the spectrum are required to represent fully a real 2-D signal. Therefore in the DT CWT [13, 14] we also filter with complex conjugates of the row (or column) filters in order to retain a second (or fourth) quadrant of the spectrum. This then gives 4 : 1 redundancy in the transformed 2-D signal. If the signal exists in *m* dimensions, further conjugate pairs of filters are needed for each additional dimension, leading to a redundancy of 2^m : 1. This process is discussed in more detail in [9]. Complex filters in multiple dimensions can provide true directional selectivity, despite being implemented separably, because they are still able to separate all parts of the *m*-D frequency space. For example a 2-D CWT produces six band pass sub images of complex coefficients at each level, which are strongly oriented at angles of $\pm 15^\circ$, $\pm 45^\circ$, $\pm 75^\circ$, as illustrated by the level 4 impulse responses in fig. 10. In order to obtain these directional responses, it is necessary to interpret the scaling function (low pass) coefficients from the two trees as

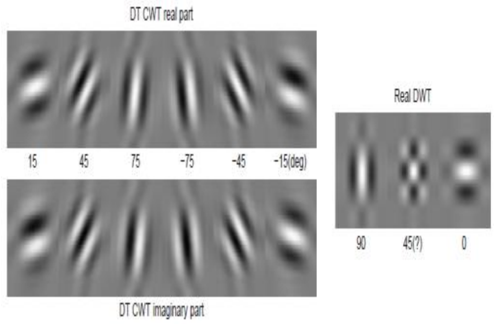

Fig 10: Impulse responses of 2-D complex wavelet filters (left), and of 2-D real wavelet filters (right), all illustrated at level 4 of the transforms.

The complex wavelets provide 6 directionally selective filters, while real wavelets provide 3 filters, only two of which have a dominant direction. Complex pairs (rather than as purely real coefficients at double the rate) so that they can be correctly combined with wavelet (high pass) coefficients from the other dimension, which are also complex, to obtain the filters oriented at $\pm 15^\circ$ and $\pm 75^\circ$. The type C wavelet filters were used in this case. It is interesting to note that *m*-dimensional CWTs will produce $(4^m - 2^m)/2$ directional band pass sub bands at each level. In 3-D this gives 28 sub bands at each level or scale, which are selective to near-planar surfaces, corresponding to approximately equally space points on the surface of a hemisphere. In fig. 8, the shift-dependent properties of the DT CWT were compared with the DWT for one-dimensional step functions. In fig. 10, a similar comparison is made in 2-D, using the DT CWT filters of type C and the same DWT as in table 3. The input is now an image of a light circular disc on a dark background. The upper row of images, from left to right in fig. 10, show the components of the output image, reconstructed from the DT CWT wavelet coefficients at levels 1, 2, 3 and 4 and from the scaling function coefficients at level 4. The lower row of images show the equivalent components when the fully decimated DWT is used instead. In the lower row, we see substantial aliasing artifacts, manifested as irregular edges and stripes that are almost normal to the edge of the disc in places. Contrast this with the upper row of DT CWT images, in which artifacts are virtually absent. The smooth and continuous images here demonstrate good shift invariance because all parts of the disc edge are treated equivalently; there is no shift dependence. These images also show good rotational invariance, because each image is using coefficients from all six directional sub bands at the given wavelet level. The only rotational dependence is a slight thinning of the rings of the band pass images near orientations of $\pm 45^\circ$ and $\pm 135^\circ$, due to the diagonal sub bands having higher centre frequencies than the others.

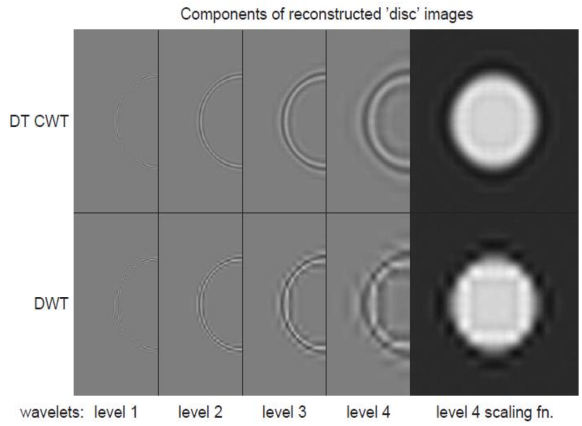

Fig 11: Wavelet and scaling function components at levels 1 to 4 of an image of a light circular disc on a dark background, using the 2-D DT CWT (upper row) and 2-D DWT (lower row). Only half of each wavelet image is shown in order to save space.

The practical advantages of shift invariant transforms become more obvious if one considers what happens to the reconstructed version of an image, such as the disc in fig. 10, when some of the wavelet sub bands are scaled differently from others. This may be a reduction in gain to achieve denoising or an increase in gain to achieve deblurring. With unity gain for all sub bands, summation of either row of images in fig. 11 produces a perfectly reconstructed disc; but with *unequal* gains, the artifacts of the lower row will tend to appear, while the upper row will just result in uniform blurring or sharpening of edges. Furthermore, by applying gain changes selectively to differently oriented sub bands of the CWT, it is possible, for example, to denoise along an edge while sharpening in a direction normal to it.

VII. IMAGE FUSION USING DWT

The discrete wavelet transform decomposes the image into low-high, high-low, high-high spatial frequency bands at

ISSN: 2277-3754
ISO 9001:2008 Certified
International Journal of Engineering and Innovative Technology (IJEIT)
Volume 3, Issue 3, September 2013

different scales and the low-low band at the coarsest scale. The L-L band contains the average image information whereas the other bands contain directional information due to spatial orientation. Higher absolute values of wavelet coefficients in the high bands correspond to salient features such as edges or lines. With these premises, Li et al. [11] propose a selection based rule to perform image fusion in the wavelet transform domain. Since larger absolute transform coefficients correspond to sharper brightness changes, a good integration rule is to select, at every point in the transform domain, the coefficients whose absolute values are higher. This idea is represented in Figure 12. Many other researchers, such as Chipman et al. [19], Koren et al. [13], Nuñezet al. [15],[17], Bogdan et al. [3] or Gomez et al. [29], have proposed different approaches to wavelet domain fusion. The common element idea in almost all of them is the use of wavelet transform to decompose images into a multiresolution scheme. Then, with some specific rules of decision or weighting, the images are combined into a single fused one. In this research it was implemented the simplest of these approaches suggested by Li et al.

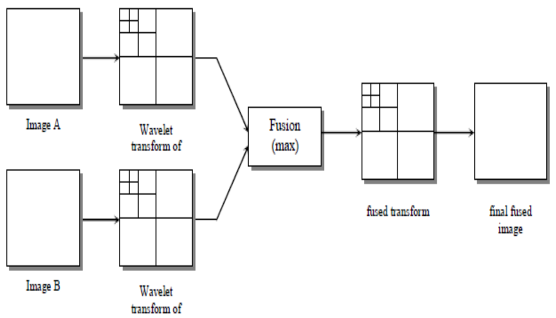

Fig 12: DWT Fusion Scheme

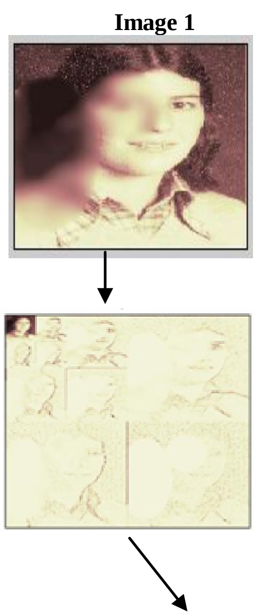

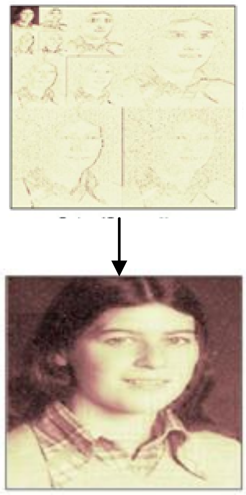

Fig 13: Image fusion process using the DWT and two registered multi-focus Catherine images

VIII. IMAGE FUSION USING CWT

Because of improved directional selectivity and shift invariant property of complex wavelet transform it is found that CWT based filter is most suitable for image fusion application. In figure 14 we have demonstrates the fusion of two images using the complex wavelet transform [11], [12]. The areas of the images more in focus give rise to larger magnitude coefficients within that region. A simple maximum selection scheme is used to produce the combined coefficient map. The resulting fused image is then produced by transforming the combined coefficient map using the inverse complex wavelet transform. The wavelet coefficient images show the orientation selectivity of the complex wavelet sub bands. Each of the clock hands which are pointing in different directions are picked out by differently oriented sub bands. We have implemented the same three fusion rules with the complex wavelet transform A complex wavelet transform was used with the filters given in [Kingusbury,2000] designed for improved shift invariance.

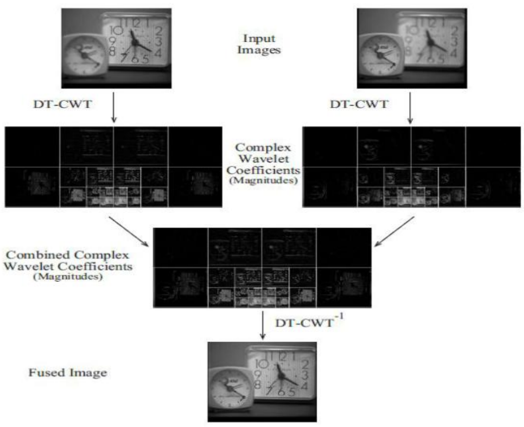

Fig14: The image fusion process using the DT-CWT and two registered multi-focus clock images.

ISSN: 2277-3754
ISO 9001:2008 Certified
International Journal of Engineering and Innovative Technology (IJEIT)
Volume 3, Issue 3, September 2013

IX. RESULTS

The performance of DWT fusion method and CWT fusion methods are compared by considering two different color images of Catherine 1(Left corrupted) and Catherine 2 (Right Corrupted) . The Synthesized image after DTT fusion method and CWT based fusion methods are a shown in figures (15) and (16) respectively. It has been observed from figure(16) that the CWT fusion techniques provide better quantitative and qualitative results than the DWT at the expense of increased computation. The CWT method is able to retain edge information without significant ringing artifacts. It is also good at faithfully retaining textures from the input images. All of these features can be attributed to the increased shift invariance and orientation selectivity of the CWT when compared to the DWT. Hence it has been demonstrated with the help of results that CWT is an essential tool for image fusion and de-noising. Due to improved directive and shift invariant properties of CWT fusion method outperforms the DWT fusion method.

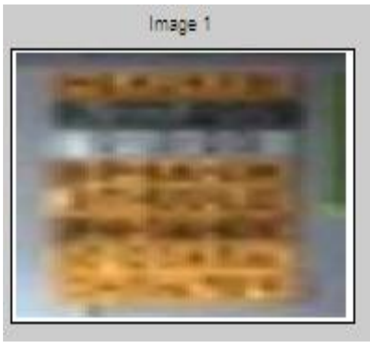

Text Image 1

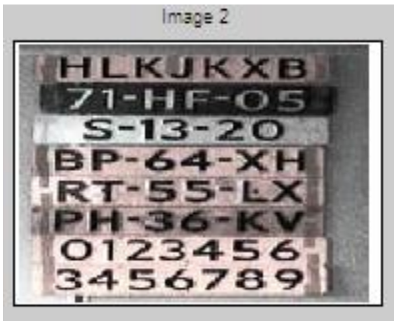

Text Image 2

Fig 15: Image Fusion and Synthesized image of image 1 and image 2 using DWT

Fig 17: Image Fusion and Synthesized image of image 1 and image 2 using CWT

Tree image 1

Tree image 2

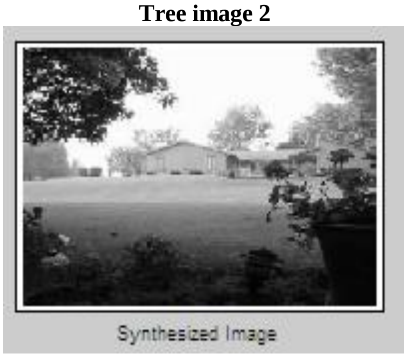

Fig 17: Image Fusion and Synthesized image of image 1 and image 2 using DWT

Fig 18: Image Fusion and Synthesized image of image 1 and image 2 using CWT

ISSN: 2277-3754
ISO 9001:2008 Certified
International Journal of Engineering and Innovative Technology (IJEIT)
Volume 3, Issue 3, September 2013

Table 2: Comparison evaluation between DWT and CWT for three different images

Images	Text Image		Catherine Image		Tree Image	
	PSNR	NCC	PSNR	NCC	PSNR	NCC
DWT	27.63	0.81	18.54	0.81	20.39	0.88
CWT	32.54	0.96	30.46	0.97	31.18	0.98

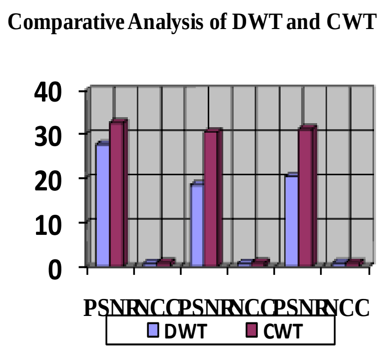

Fig 19: Comparative analysis of DWT and CWT of three different images Text, Catherine and Tree

X. CONCLUSION

The objective of this work has been to propose a complex wavelet transform based filter. The comparative analysis between complex wavelet transforms fusion methods CWT with the existing fusion techniques. For an effective fusion of images a technique should aim to retain important features from all input images. These features often appear at different positions and scales. Multi resolution analysis tools such as the complex wavelet transform are ideally suited for image fusion. Simple DWT methods for image fusion have produced limited results. The sub-sampling structure is not very symmetrical. The two trees have slightly different frequency responses. The filter sets must be biorthogonal because they are linear phase. The CWT fusion technique for test images text and tree provides better results than the DWT fusion technique as depicted in figure (14) and figure (15). The CWT based fusion method is able to retain important edge information without significant humming artifacts. CWT provides increased shift-invariance and orientation selectivity when compared to the DWT. This is demonstrated and furnished in table2 shown above. The above figure (22) shows the analysis and performance of DTCWT and QDTCWT for three test images of Text, Catherine and Tree image.

XI. ACKNOWLEDGMENT

The authors would like to thank N. G. Kingsbury, from the University of Cambridge, for providing the DWT and CWT code for Matlab and Oliver Rockinger from Metapix, for providing the image fusion toolbox for Matlab without that it is not possible for us to proceed our research in this field.

REFERENCES

[1] G. Strang and T Nguyen, Wavelets and Filter Banks, Wellesley-Cambridge Press, Wellesley MA 02181 USA, 1997.

[2] M. Antonini, M. Barlaud, P. Mathieu, and I. Daubechies, Image Coding Using the Wavelet Transform, IEEE Trans on Image Processing, 2(2) , Pages 205-220, April 1992.

[3] M. J. T. Smith and T. P. Barnwell, Exact Reconstruction Techniques for Tree-Structured Sub band Coders, IEEE Transactions ASSP, 34, Pages 434-441, 1986.

[4] S G Mallat, “A theory for multiresolution signal decomposition: The wavelet representation”, IEEE Trans. PAMI, 11(7), pp 674-693, 1989.

[5] N G Kingsbury, “The dual-tree complex wavelet transform: a new technique for shift invariance and directional filters”, Proc.8th IEEE DSP Workshop, Bryce Canyon, Aug 1998.

[6] N G Kingsbury: “The dual-tree complex wavelet transform: a new efficient tool for image restoration and enhancement”, Proc. EUSIPCO 98, Rhodes, Sept 1998.

[7] J F A Magarey and N G Kingsbury, “Motion estimation using a complex-valued wavelet transform”, IEEE Trans. Signal Proc., 46(4), April 1998.

[8] D B H Tay and N G Kingsbury, “Flexible design of multidimensional perfect reconstruction FIR 2-band filters using transformations of variables”, IEEE Trans. Image Proc., 2(4), pp 466-480, 1993.

[9] N G Kingsbury: “Image processing with complex wavelets”, Phil. Trans. Royal Society London A, September 1999, Special issue for the discussion meeting on “Wavelets: the key to intermittent information?” (held Feb 24-25, 1999), 357, pp 2543-2560.

[10] Resources for research in image fusion :[Online], http://www.imagefusion.org/

[11] The Math works, „Wavelet Toolbox (ver 5) User’s guide 2007, URL: www.mathworks.com

[12] H.B. Mitchell. Image Fusion theories, techniques, and applications”, ISBN 978-642-11215-7, Springer-Verlag Berlin Heidelberg, 2010.

[13] N G Kingsbury: “Shift invariant properties of the Dual-Tree Complex Wavelet Transform”, Proc. ICASSP 99, Phoenix, AZ, paper SPTM 3.6, March 16-19, 1999.

[14] J Romberg, H Choi, R Baraniuk and N G Kingsbury: Multiscale classification using complex wavelets”, Proc. ICIP 2000, Vancouver, Sept 2000.

AUTHOR’S PROFILE

Rudra Pratap Singh Chauhan B. TECH. (ELECTRONICS and COMMUNICATION), M. TECH (ELECTRONICS and COMMUNIATION), pursuing P. hd. in the field of Image processing application. The author has total fourteen research paper in the field of image processing.

ISSN: 2277-3754
ISO 9001:2008 Certified
International Journal of Engineering and Innovative Technology (IJEIT)
Volume 3, Issue 3, September 2013

Dr. Rajiva Dwivedi, M. SC., M. TECH in RF Microwave and Antenna, P hd, from IT BHU, having more than fifty research paper in international journals.